On interface dipole layers between C60 and Ag or Au

Veenstra, Sjoerd; Heeres, A.; Hadziioannou, G.; Sawatzky, G.A.; Jonkman, H.T.

Published in:
Applied Physics A%3A Materials Science %26 Processing

DOI:
10.1007/s003390201311

Publication date:
2002

Appl. Phys. A 75, 661–666 (2002)
DOI: 10.1007/s003390201311

Applied Physics A
Materials Science & Processing

S.C. VEENSTRA[1]
A. HEERES[2]
G. HADZIIOANNOU[1]
G.A. SAWATZKY[2]
H.T. JONKMAN[2,✉]

On interface dipole layers between C_{60} and Ag or Au

[1] Department of Polymer Chemistry, Materials Science Centre, University of Groningen, Nijenborgh 4, 9747 AG Groningen, The Netherlands
[2] Laboratory of Solid State and Applied Physics, Materials Science Centre, University of Groningen, Nijenborgh 4, 9747 AG Groningen, The Netherlands

Received: 26 September 2001/Accepted: 15 January 2002
Published online: 3 June 2002 •

ABSTRACT C_{60} layers on polycrystalline Ag and Au are studied by photoelectron spectroscopy. At these metal/C_{60} interfaces an electron transfer occurs from the metal to the lowest unoccupied orbital of C_{60}. We found in the case of the polycrystalline Ag/C_{60} interface a dipolar layer with its associated electric field in the direction corresponding to the charge transfer, so pointing from the substrate to the adsorbent. Yet, at the Au/C_{60} interface we observed an overall electric field pointing from C_{60} towards the metal. We discuss our observations in terms of charge transfer, screening and hybridization effects and propose the occurrence of a hybridization mechanism similar to back-bonding at the Au/C_{60} interface. We show that the alignment of energy levels at the metal/C_{60} interface cannot simply be deduced using the metal workfunction and the frontier orbitals of C_{60}, including screening effects, since hybridization effects may strongly alter the interfacial energy level structure. Our experimental findings on the polycrystalline metal/C_{60} interfaces indicate an at-most weak dependence of the Fermi level of the C_{60} overlayer on the workfunction of the polycrystalline metal substrate. These interfaces are found in donor–acceptor-based organic photovoltaic devices and our results may help to understand the electrical characteristics of these devices.

PACS 33.15.Ry; 73.30.+y; 73.61.Wp

1 Introduction

Organic semiconducting materials have attracted a lot of attention in the scientific community, because of their interesting physics and potential applications in light-emitting devices (LEDs), field-effect transistors (FETs) and photovoltaic devices (PVDs). In order to understand the electrical device properties of these organic semiconductors, direct measurements of the relevant energy levels for charge transport are valuable. These levels include the workfunctions of the metal electrodes, the highest occupied molecular orbital (HOMO) and the lowest unoccupied molecular orbital (LUMO) of the organic semiconducting materials. Besides the absolute values of these energy levels, also their mutual alignment at interfaces is important, since it was recently shown that the use of the so-called vacuum-level alignment principle may lead to erroneous results [1–4]. The misalignment of the vacuum levels is caused by interfacial dipole layers whose mechanism is not completely understood.

Of all the organic semiconducting materials C_{60} is of special interest because of the spectacular results obtained with this material in PVDs and in FETs. In PVDs, C_{60} acts as a very efficient electron acceptor, stabilizing the meta-stable charge-separated state after the fast (sub-picosecond) photoinduced electron transfer from the electron donor [5–7]. In FETs based on C_{60}, switching is possible from an insulating to a superconducting state, with a transition temperature, T_c, peaking at 52 K [8, 9].

In these devices, interfaces play an important role: in FETs, charges are induced in the organic layer closest to the gate. So, the conduction channel is not somewhere in the bulk, but confined to a thin layer at the organic/insulator interface. In bulk heterojunction-based PVDs the photoinduced charge transfer occurs at the donor/acceptor interface. In both types of devices, as well as in LEDs, the metal/organic interface is important since the charges have to cross it under device operation.

In organic PVDs the origin of the so-called open-circuit voltage (V_{oc}) is not well understood. The experimental indications are that the V_{oc} is nearly independent of the metal-electrode workfunction, which is contrary to what one naively would expect. Therefore we decided to investigate the energy-level alignment at polycrystalline Ag/C_{60} and Au/C_{60} interfaces, since these are the actual metal electrodes in the devices.

Energy levels at interfaces may deviate substantially from the bulk due to the asymmetry in their environment resulting in a different polarization of the surrounding medium. To indicate the importance of the environment on the molecular orbital structure, Fig. 1 shows the electron affinity (E_A) and the ionization potential (E_I) of C_{60} in three different systems: as isolated molecule (A), on the surface of bulk C_{60} (B) and in a monolayer of C_{60} on a Ag surface (C). The energy difference between E_A and E_I (the conductivity gap) is reduced by a factor of 2 when comparing the energy levels of an isolated molecule with those of a C_{60} monolayer on Ag (111).

✉ Fax: +31-50/363-4879, E-mail: jonkman@phys.rug.nl

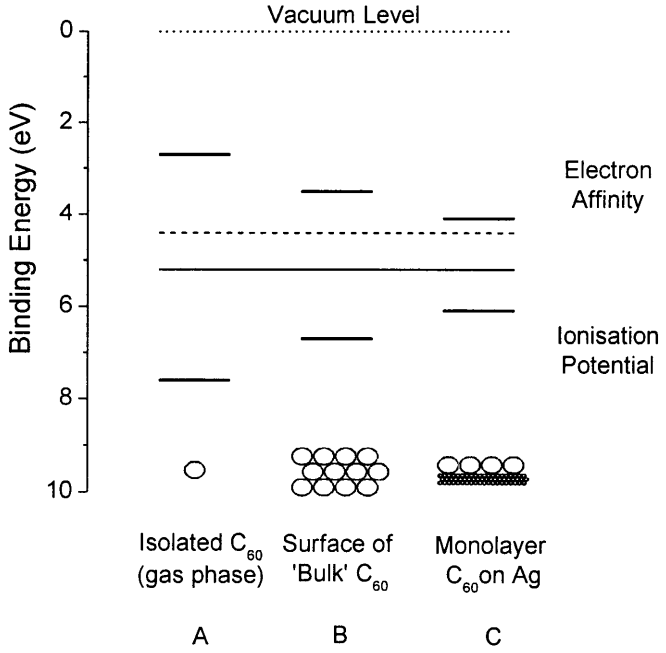

FIGURE 1 Dependence of the electron affinity and ionization potential of C_{60} on screening effects (using Franck–Condon maximum). The lines indicates the position of the workfunction of polycrystalline Ag (~ 4.4 eV), the continuous line indicates the workfunction of polycrystalline Au (~ 5.2 eV). Values taken from [13, 21, 34–39]

In the system depicted by Fig. 1c, the metal stabilizes the charged state of the C_{60}-ion, since the metal effectively screens the ion. This screening may be understood by using the image potential model [10]. The stabilization of the C_{60}-ion by this polarization effect increases the electron affinity to approximately 4 eV, a value close to the workfunction of common metals. If we take into account that the width of the lowest unoccupied molecular orbital (LUMO) of C_{60} is approximately 1 eV and assume vacuum level alignment for the moment, we can anticipate that the lowest unoccupied molecular orbital of C_{60} on metals with a workfunction of around 4.5 eV or lower may be partially filled [11]. This is indeed observed for C_{60} deposited on Ag [12]. However, when C_{60} is deposited on Au with a workfunction of around 5.2 eV one can also observe a partial electron transfer from the metal to C_{60} [12]. Such a process seems unlikely to occur if the vacuum levels on both sides of the interface are aligned, see Fig. 1. Many metal/C_{60} interfaces have been studied and substantial workfunction changes have been observed (see for example [13–17]). At these interfaces electron transfer from the metal substrate to the C_{60} monolayer was observed but the charge transfer could not explain the observed workfunction change of the C_{60} overlayer. The authors explain their observations by the supposed metallic nature of the C_{60} overlayer, making the workfunction of the C_{60} overlayer independent of the metal substrate. Although this does not explain the observed differences in workfunction of the C_{60} overlayer of 4.7 eV for C_{60} on Au (111) [18], 5.25 eV for C_{60} monolayer on Al (110) [15] and 5.4 eV for a C_{60} overlayer on Ta [19].

Here we report on interfaces formed by depositing C_{60} on polycrystalline Ag and Au films. First we discuss the polycrystalline Ag/C_{60} interface and explain the observations in terms of screening effects and interfacial charge transfer. This interface is adequately described elsewhere [10, 12], and is mainly used here as a reference. Second, we discuss the polycrystalline Au/C_{60} interface and come to the conclusion that the spectra cannot be explained using the same concepts. We propose an explanation for the experimental findings on the polycrystalline Au/C_{60} interface by describing three interacting effects. First, a screening effect of the metal-substrate reducing of the on-site Coulomb interaction leading to a reduction of the energy gap between occupied and unoccupied levels. Second, broadening of the spectral features due to hybridization between the Au 6*sp*-band and the occupied π and unoccupied π^* orbitals of C_{60}. The combination of the reduced gap and the spectral broadening results in an electron transfer from the metal substrate to the C_{60} LUMO. Third, a dipole field at the Au/C_{60} interface caused by the deposition of C_{60} onto the clean Au surface. The adsorbed C_{60} molecules redistribute the Au 6*sp* electrons whose wavefunctions extent far into the vacuum prior to the adsorption of C_{60} to the substrate. This redistribution causes a dipole layer in the first Au layer. This field opposes the electric field caused by the electron transfer from the metal substrate to C_{60}. Further we speculate that hybridization occurs between the Au 6*sp*-band via the Au 5*d*-band with the valence orbitals of C_{60} in a process that resembles back-bonding, a mechanism found in organo-metallic complexes.

2 Experimental

All experiments were performed in a UHV system consisting of an entry-lock, a preparation chamber (with a base pressure $< 2 \times 10^{-9}$ mbar) and a measurement chamber (with a base pressure in the low 10^{-10} mbar). The preparation chamber was equipped with a C_{60} evaporation cell of our own design, a layer-thickness monitor (Sycon instruments, STM-100), a sample annealing stage and a Knudsen cell for Au depositions. Clean polycrystalline Au films were prepared in situ by deposition of Au (thickness > 50 nm) on a cleaned Si-wafer. Metal strips clamped the Si-wafer to a metal sample plate assuring a good electrical contact between the gold film and the sample plate.

Polycrystalline Ag substrates were directly mounted on the sample plate and thoroughly cleaned by polishing and washing in an ultrasonic bath with toluene and acetone as solvents. Next, the Ag substrates were inserted in the preparation chamber where they were sputtered to obtain clean polycrystalline surfaces. Ultraviolet photoemission spectroscopy (UPS) was used to check the cleanliness of the metal substrates. During C_{60} deposition the pressure in the preparation chamber increased to around 5×10^{-8} mbar. C_{60} monolayers on Au were prepared using a distillation procedure described elsewhere [20].

UPS was carried out in a separate chamber using a combined UPS/XPS measurement system (Vacuum Generators). UPS spectra were taken with He-I radiation ($h\nu = 21.22$ eV) with an overall resolution of 0.15 eV. All spectra were corrected for the contribution of the He-I satellite.

For the workfunction measurements, the sample was biased to -3.00 or -4.00 V to improve the onset of the spectrum in the low-kinetic-energy region (secondary-electron

cut-off). The position of the peak onsets and the secondary-electron cut-offs were determined by the intersection of the tangents of the peak and the baseline. Peak positions were determined by peak-fitting the experimental data to a Gaussian function.

3 Results and discussion

3.1 C_{60} *on* Ag

Figure 2a shows the UPS spectra of polycrystalline Ag and of a C_{60} layer (several nanometers thick) deposited on the Ag substrate. The energy diagram deduced from these spectra is displayed in Fig. 2b.

The shift of the low-kinetic-energy onset of the spectrum (the secondary-electron cut-off), which is shown in detail in the inset of Fig. 2a, determines the vacuum-level shift of -0.133 eV as shown in Fig. 2b. The shift is caused by an electric field at the Ag/C_{60} interface. The direction of the electric field is such that Ag substrate is somewhat positively, and C_{60} negatively, charged.

The energy difference between the Fermi level of Ag and the LUMO of C_{60} is 0.25 eV. The HOMO–LUMO gap at the metal/C_{60} interface is reduced by more than 0.5 eV due to screening effects [21], and this causes the LUMO orbital to move downward, see Fig. 1b and c. As soon as the onset of the LUMO shifts below the Fermi level of Ag, electrons will be injected from the metal into the LUMO of the C_{60}. When electrons start populating the C_{60} unoccupied orbitals, an electric field is created at the Ag/C_{60} interface, which lifts the energy levels of the organic layer relative to those of the metal substrate. In this way the system reaches equilibrium.

Note that only the LUMO of the first (two) C_{60} monolayer(s) on the metal accept(s) electrons from the metal substrate, since the stabilizing effect of the image charge decreases with $1/r$, where r is the distance between the charge and the metal surface. This confinement of the charges at the Ag/C_{60} interface is also found experimentally in the UPS spectra: in Fig. 2a the spectrum of the C_{60} layer of several nm thick (so, several monolayers thick) contains no spectral weight close to the Fermi level. However in the UPS spectrum of a *monolayer* of C_{60} on polycrystalline Ag, a clear spectral feature is present around the Fermi level of the metal [12].

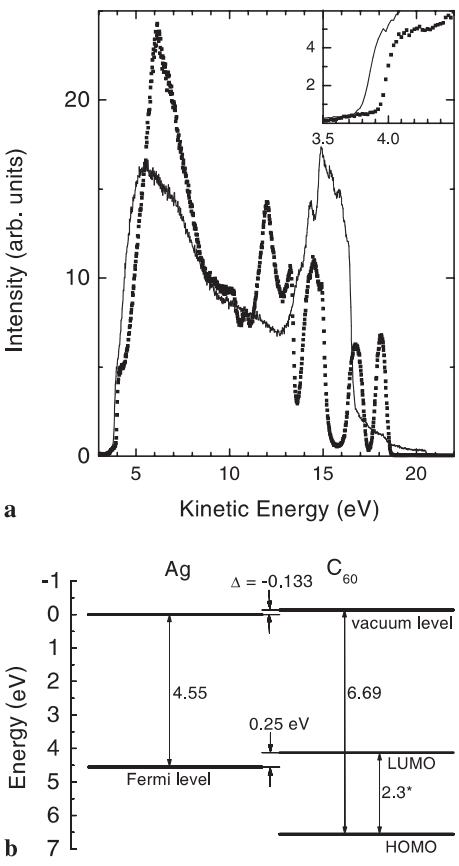

FIGURE 2 **a** UPS spectra of polycrystalline Ag (*line*) and of a several-nanometer-thick layer of C_{60} deposited on polycrystalline Ag (*square symbols*). **b** Energy-level diagram of the alignment of energy levels between polycrystalline Ag and bulk C_{60} deduced from both UPS spectra shown in **a**. The HOMO–LUMO gap is taken from [37], where the energy difference is taken from the onset of the HOMO to the onset of the LUMO instead of the peak-to-peak value

3.2 C_{60} *on* Au

The UPS spectra of Au, a monolayer of C_{60} on Au and a C_{60} layer of 5 to 10 nm on Au are shown in Fig. 3a. The left panel shows the misalignment (of around 0.6 eV) between the secondary-electron cut-off of Au on one hand and the cut-offs of the C_{60} monolayer and the thicker C_{60} film on the other. The inset on the right-hand side shows the UPS spectra close to the Fermi level.

We first note the above-mentioned misalignment between the low-kinetic-energy onset of the Au spectrum compared to the same onsets of the C_{60} spectra. Second, the low-binding-energy features in the spectrum (HOMO and HOMO-1) of the C_{60} monolayer are broadened *and* shifted to lower binding energy when compared to the spectrum of the 'bulk' C_{60} film (right inset). Third, we note an increase in spectral weight around the Fermi energy of the Au substrate in the spectrum of the C_{60} monolayer, which is absent in the 'bulk' C_{60} spectrum. Finally, we note by closer inspection of the right-hand inset of Fig. 3a that the values of the decrease in binding energy of the HOMO and the HOMO-1 of the C_{60} monolayer relative to the positions found for the C_{60} 'bulk' are not identical. The shift of the HOMO peak is larger (0.3 eV) compared to the shift of the HOMO-1 (0.2 eV), therefore this is not a rigid shift.

Figure 3b represents the energy level diagram deduced from the spectra reported in Fig. 3a.

The first observation, the shift of the secondary-electron cut-off of the UP spectra of C_{60} to lower kinetic energy compared to the onset of the UPS spectrum of Au, shows similarities with other Au/organic interfaces [1, 4, 22]. The general trend at these interfaces is a shift of the secondary-electron cut-off of the organic layer, to lower kinetic energies. Generally, this shift is a rigid shift, caused by an interfacial dipolar layer, moving all energy levels of the absorbent downward relative to the levels of the Au substrate [1, 4, 22]. The dipole originates from a polarization of the interface due to redistribution of the electrons at the interface upon the interface formation. It is known that the electron distribution at the Au surface extends rather far into the vacuum, this is known as a 'spill-out' [23]. A plausible explanation may be that upon absorption of a molecule to the Au surface, these electrons

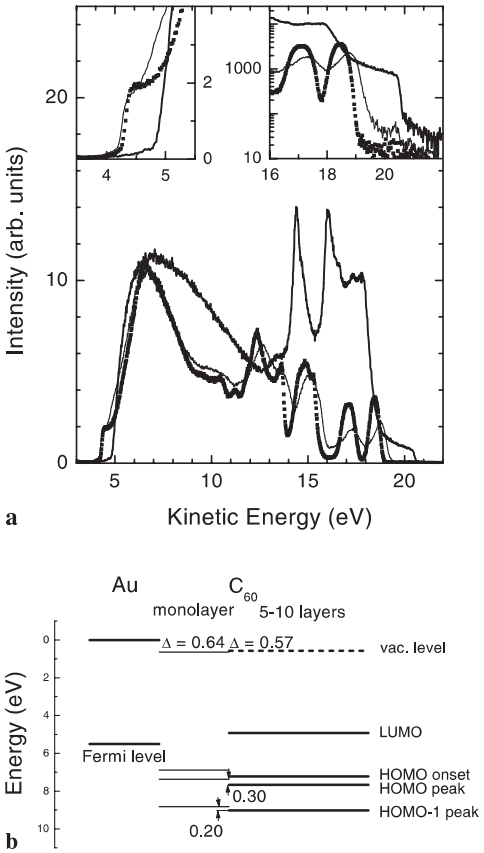

FIGURE 3 **a** UPS spectra of a polycrystalline Au substrate (*thick continuous line*), a monolayer of C_{60} on the Au substrate (*thin continuous line*) and layer of C_{60}, several nanometers thick (*square symbols*). The *left inset* shows in detail the secondary-electron cut-offs of the three spectra, the *right-hand inset* is an enlargement of the spectral features close to the Fermi level on a semilog scale. **b** Energy level diagram of the interface between Au and C_{60} deduced from the UPS spectra shown in **a**.

are pushed back somewhat to the Au bulk, and this redistribution of electrons at the interface causes the local field. We will comment on this below.

The second observation concerns the shift and broadening of the low-binding-energy features (HOMO and HOMO-1) in the C_{60} monolayer spectrum compared to the C_{60} 'bulk' spectrum. The shift of these features to lower binding energy is explained using the concept of 'image charge': the ionization of a C_{60} molecule at the Au surface requires less energy due to the more effective screening of the C_{60}-ion in the final state by the presence of the highly polarizable metal surface. Due to the same effect the electron affinity increases: in other words, the HOMO–LUMO gap drastically decreases.

The broadening of the same low-binding-energy features is attributed to hybridization between π- and π^*-orbitals of the C_{60} molecules in the first monolayer with the Au 6*sp*-band of the Au substrate. The combination of the lowering of the LUMO due to screening effects and the broadening of the LUMO due to hybridization effects causes the onset of the LUMO to move below the Fermi level of the metal substrate. This leads to a partial filling of the LUMO of the C_{60} monolayer, and explains the increase in spectral weight near the Fermi energy of the metal substrate.

So far, the explanation for the polycrystalline Au/C_{60} interface also applies to the polycrystalline Ag/C_{60} interface. However, now we arrive at an important difference between the two metal/C_{60} interfaces. At the Ag/C_{60} interface an electric field exists, pointing from the metal ($\delta+$) to C_{60} ($\delta-$), as indicated by the shift of the secondary-electron cut-off in Fig. 2a. This is consistent with the partial electron transfer from the metal to the LUMO of C_{60} that is observed [12]. The low-kinetic-energy onsets of the spectra of Au and C_{60}, Fig. 3a, imply an electric field pointing from C_{60} ($\delta+$) towards the Au substrate ($\delta-$). This seems to contradict the partial filling of the LUMO of the C_{60} monolayer by electron transfer from the Au substrate to the organic layer, as was already reported for C_{60} monolayers on several crystalline metal substrates [13, 15–17]. These authors argue that the C_{60} overlayer acts as a metal and that the image plane moves from the interface to the outside of the C_{60} overlayer. Any interface dipole layer between the metal substrate and C_{60} caused for example by the electron transfer from the substrate to C_{60} is screened out by the image plane. The workfunction of the metallic C_{60} overlayer is expected to be a material property and therefore independent of the metal substrate. However this does not explain the observed differences in workfunction of the C_{60} overlayer of 4.7 for C_{60} on Au(111) [18], 5.25 for C_{60} monolayer on Al(110) [15] and 5.4 for a C_{60} overlayer on Ta [19].

We start our explanation by recalling that the chemical potential on either side of the interface should be equal if the interface is in its equilibrium state. Normally this requires charge redistribution at the interface between two different materials. For example, at interfaces between two metals this leads to a contact potential, in inorganic semiconductors this requirement causes band-bending by sweeping excess charges from the depletion layer to the interface.

In the system formed by polycrystalline Ag and a C_{60} overlayer, we see that the energy of the LUMO of the C_{60} monolayer and the Fermi level of Ag almost coincide if the vacuum levels would align at this interface (see Fig. 1). In order to reach chemical equilibrium, a charge redistribution will occur causing an partial electron transfer to the C_{60} overlayer. In the case of the interface formed by a monolayer of C_{60} on polycrystalline Au, the Fermi level of the metal is close to the middle of the HOMO–LUMO gap of the C_{60} overlayer if we again assume vacuum-level alignment. A charge redistribution at this interface by transferring electrons from the metal to unoccupied levels in C_{60} seems unlikely since there are no levels available close to the Fermi level of the substrate.

We continue our explanation by looking at a system consisting of a clean Au surface and an isolated C_{60} molecule far from this surface, see Fig. 4, top panel. The electron distribution of C_{60} is spherical symmetric without permanent dipoles. The metal surface on the other hand shows an asymmetric charge distribution, due to the spill-out of the Au 6*sp*-electrons that occupy wavefunctions, which extend far into the vacuum. In this way a permanent dipole exists at this surface; actually it is this dipole that gives an important contribution to the workfunction of the metal.

Now we let the molecule approach the Au substrate. This causes a (Born) repulsion between electrons at the Au sub-

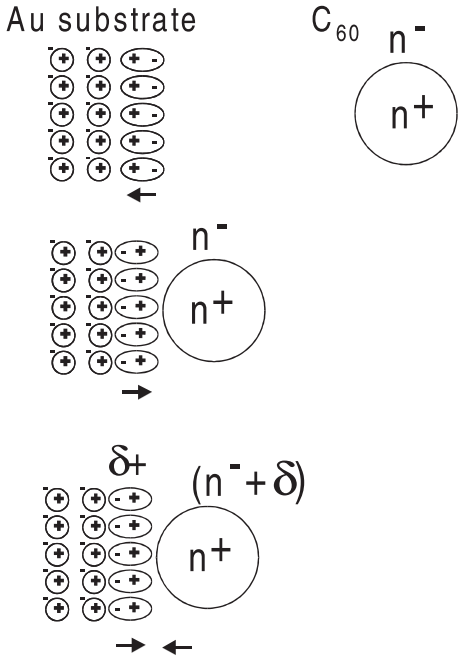

FIGURE 4 Schematic of a redistribution of electron density at the interface formed upon the deposition of a monolayer of C_{60} onto a gold surface. The *bold arrows* indicate the presence and orientation of a dipole field. *Top panel* represents a clean Au substrate surface and an isolated C_{60} molecule far from this metal surface, both in vacuum. At the Au/vacuum interface a dipole exists mainly due to the asymmetric Au 6*sp*-orbitals that extend far into the vacuum. The *middle panel* shows a redistribution of the Au 6*sp*-orbitals upon the interface formation between C_{60} and Au. The *bottom panel* depicts the final state in which a partial electron transfer occurs between the Au substrate and the C_{60} overlayer

strate and electron of the C_{60} molecule. Since the spatial distribution of the Au 6*sp*-electrons is easily altered, these electrons will be pushed back towards the substrate, thus changing the initial surface dipole. (Fig. 4, middle panel). This change of the dipole may be (partially) compensated by the electron transfer from the metal substrate to the LUMO of C_{60} (Fig. 4, bottom panel).

In retrospect we think that the same processes occur at the polycrystalline Ag/C_{60} interface, however, in this system it does not lead to an overall dipole in the opposite direction as inferred from the observed electron transfer.

We can speculate as to what extent hybridization plays a role at the metal–C_{60} interface.

By comparing the UPS spectra of the C_{60} 'bulk' with the C_{60} monolayer (Fig. 3a) we note an unequal shift of the two lowest-binding-energy features (the fourth observation). We attribute the unequal shift to differences in hybridization between states contributing to the HOMO and HOMO-1 of C_{60} with the Au 5*d*-band of the substrate.

These hybridization differences originate from differences in overlap between the Au 5*d*-band and the low-binding-energy orbitals of C_{60}. These differences may become clear by comparing the UPS spectra of a C_{60} monolayer on polycrystalline Au and on polycrystalline Ag (Fig. 1, in [20] and Fig. 3 in this paper). The valence orbital structure of a monolayer C_{60} on Ag is hardly changed when compared to the 'bulk' C_{60} spectrum, except for effects leading to the partial filling of the LUMO. Hybridization between the Ag 4*d*-band and the C_{60} HOMO is not anticipated to be important since these states are well separated in energy.

On the other hand, the HOMO and the HOMO-1 of C_{60} overlap nicely with the Au 5*d*-band and in the UPS spectrum of the C_{60} monolayer on polycrystalline Au, we observe that these π-orbitals (HOMO and HOMO-1) are distorted. Therefore we anticipate that the metal *d*-band plays an important role in the hybridization between the metal substrate and the C_{60} monolayer. Most likely the anticipated hybrid bond is a combination of the Au 5*d*- and Au 6*sp*-bands with the π-orbitals of C_{60}. Such a hybridization of orbitals between the Au and C_{60} leads to a different occupation of the states close to the Fermi level, which leads to a shift in electron density from the C_{60} monolayer to the Au substrate.

This electron redistribution resembles a process often found in organo-metallic (OM) complexes, known as back-bonding, or back-donation [24–26]. These complexes are intensively studied since they are of fundamental interest in organo-metallic chemistry and have important applications in the field of catalysis [24–27].

The hybridization between C_{60} and polycrystalline Au shows correspondence with the back-bonding mechanism. The donation step occurs through partial filling of the LUMO by hybridization between the Au 6*sp*-band with π^*-orbital of C_{60}. The back-bonding step stems from hybridization between the HOMO of C_{60} via the Au 5*d*-band with the Au 6*sp*-band. In order to determine the different contributions of screening and hybridization effects at a specific metal/C_{60} interface, experiments on metal single-crystal surfaces should be done.

If the proposed mechanism is proven to be correct it will have important implications for organic semiconductor devices. The alignment of energy levels on both sides of the interface will depend on the specific combination of materials *and* of the relative orientation of both components towards each other. An interesting example of the importance of the metal-crystal surface for the interfacial electronic structure was recently reported by Cepek et al. [28], who observed a temperature-dependent Fermi gap opening at the interface formed by Ag (100)/C_{60}. The authors did not observe this effect at the Ag (110)/C_{60} interface.

Hybridization effects give a handle to tune the alignment of energy levels relevant for charge injection, for example by altering the molecular packing on the metal substrate [29], by growing epitaxial molecular layers on a particular crystal surface of a metal substrate [30], or by using an interfacial layer [31].

Finally we note that our observations are in agreement with recent experimental findings in PVDs based on blends of conjugated oligomers or polymers with C_{60}-derivatives. In one study interface dipole layers of similar magnitude were found between the C_{60} layer and the electrodes [32]. In another study it was shown that the open-circuit voltage of the PVDs was nearly independent of the metal workfunction and linearly proportional to the electron affinity of the C_{60} derivative [33]. Although the interfaces were created under different experimental conditions, the results may properly be ascribed to an alignment of the LUMO of the C_{60}-derivative to the Fermi level of the metal electrode.

4 Conclusions

We discuss the interfaces between C_{60} and polycrystalline Ag and Au. We observed a shift in the secondary-electron cut-off upon the deposition of C_{60} on both metals. The shift indicates an overall electric field at the Ag/C_{60} interface towards the adsorbent. Yet, for the Au/C_{60} interface we observed a shift pointing in the other direction. We suggest a qualitative explanation to our experimental findings for C_{60} on polycrystalline Ag and Au. We propose a subtle interplay between several interacting and opposing effects, resulting in a partial filling of the LUMO of the C_{60} monolayer and an overall interfacial dipole which can be directed from the metal to the adsorbent, as in the case of Ag/C_{60}, or from the adsorbent to the metal, as observed at the Au/C_{60} interface.

REFERENCES

1 H. Ishii, K. Sugiyama, E. Ito, K. Seki: Adv. Mater. **11**, 605 (1999)
2 I.G. Hill, A.J. Mäkinen, Z.H. Kafafi: Appl. Phys. Lett. **77**, 1825 (2000)
3 H. Proehl, M. Toerker, F. Sellam, T. Fritz, K. Leo, C. Simpson, K. Müllen: Phys. Rev. B **63**, 205 409 (2001)
4 S.C. Veenstra, U. Stalmach, V.V. Krasnikov, G. Hadziioannou, H.T. Jonkman, A. Heeres, G.A. Sawtzky: Appl. Phys. Lett. **76**, 2253 (2000)
5 N.S. Sariciftci, L. Smilowitz, A.J. Heeger, F. Wudl: Science **258**, 1474 (1992)
6 B. Kraabel, D. McBranch, N.S. Sariciftci, D. Moses, A.J. Heeger: Phys. Rev. B **50**, 18 543 (1994)
7 C.J. Brabec, G. Zerza, G. Cerullo, S. de Silvestri, S. Luzzati, J.C. Hummelen, N.S. Sariciftci: Chem. Phys. Lett. **340**, 232 (2001)
8 J.H. Schön, C. Kloc, R.C. Haddon, B. Batlogg: Science **288**, 656 (2000)
9 J.H. Schön, B. Batlogg: Nature **408**, 549 (2000)
10 R. Hesper: *The influence of surfaces and interfaces on the properties of* C_{60} *compounds, Ph.D. Thesis* (Groningen, The Netherlands 2000)
11 E. Burnstein, S.C. Erwin, M.Y. Jiang, R.P. Messmer: Phys. Scr. **142**, 207 (1992)
12 B.W. Hoogenboom, R. Hesper, L.H. Tjeng, G.A. Sawatzky: Phys. Rev. B **57**, 11 939 (1998)
13 A.J. Maxwell, P.A. Brühwiler, D. Arvanitis, J. Hasselström, N. Mårtensson: Chem. Phys. Lett. **260**, 71 (1996)
14 P. Rudolf, G. Gensterblum, R. Caudano: J. Phys. IV France **7**, C6 137 (1997)
15 A.J. Maxwell, P.A. Brühwiler, D. Arvanitis, J. Hasselström: Phys. Rev. B **57**, 7312 (1998)
16 K.-D. Tsuei, J.-Y. Yuh, C.-T. Tzeng, R.-Y. Chu, S.-C. Chung, K.-L. Tsang: Phys. Rev. B **56**, 15 412 (1997)
17 K.-D. Tsuei, P.D. Johnson: Solid State Commun. **101**, 337 (1997)
18 C.-T. Tzeng, W.-S. Lo, J.-Y. Yuh, R.-Y. Chu, K.-D. Tsuei: Phys. Rev. B **61**, 2263 (2000)
19 M.W. Ruckman, B. Xia, S.L. Qiu: Phys. Rev. B **48**, 15 457 (1993)
20 L.H. Tjeng, R. Hesper, A.C.L. Heessels, A. Heeres, H.T. Jonkman, G.A. Sawatzky: Solid State Commun. **103**, 31 (1997)
21 R. Hesper, L.H. Tjeng, G.A. Sawatzky: Europhys. Lett. **40**, 177 (1997)
22 I.G. Hill, D. Milliron, J. Schwartz, A. Kahn: Appl. Surf. Sci. **166**, 354 (2000)
23 J. Hölzl, F.K. Schulte: *Solid Surface Physics, Work Function of Metals, Springer Tracts in Modern Physics*, Vol. 85 (Springer, Berlin, Heidelberg, New York 1979)
24 M. Dewar: Bull. Soc. Chim. **18**, C79 (1951)
25 J. Chatt, L.J. Duncanson: Chem. Soc. 2939 (1953)
26 F.A. Cotton, G. Wilkinson: *Advanced Inorganic Chemistry*, 5th edn. (Wiley-Interscience, New York 1988)
27 H. Zeiss, P.J. Wheatley, H.J.S. Winkler: *Benzenoid-Metal Complexes* (The Ronald Press Company, New York 1966)
28 C. Cepek, I. Vobornik, A. Goldoni, E. Magnano, G. Selvaggi, J. Kröger, G. Panaccione, G. Rossi, M. Sancrotti: Phys. Rev. Lett. **86**, 3100 (2001)
29 L. Athouël, G. Froyer, M.T. Riou, M. Schott: Thin Solid Films **274**, 35 (1996)
30 W. Gebauer, M. Bässler, A. Soukopp, C. Vaterlein, R. Fink, M. Sokolowski, E. Umbach: Synth. Met. **83**, 227 (1996)
31 L.S. Hung, C.W. Tang, M.G. Mason: Appl. Phys. Lett. **70**, 152 (1997)
32 C. Melzer, V.V. Krasnikov, G. Hadziioannou: Chem. Phys. Lett., in press
33 C.J. Brabec, A. Cravino, D. Meissner, N.S. Sariciftci, T. Fromherz, M.T. Rispens, L. Sanchez, J.C. Hummelen: Adv. Funct. Mater. **11**, 374 (2001)
34 L.-S. Wang, J. Conceicao, C. Jin, R.E. Smalley: Chem. Phys. Lett. **182**, 5 (1991)
35 X.-B. Wang, C.-F. Ding, L.-S. Wang: J. Chem. Phys. **110**, 8217 (1999)
36 I.V. Hertel, H. Steger, J. de Vries, B. Weisser, B. Kamke, W. Kamke: Phys. Rev. Lett **68**, 784 (1992)
37 R.W. Lof, M.A. van Veenendaal, B. Koopmans, H.T. Jonkman, G.A. Sawatzky: Phys. Rev. Lett. **68**, 3924 (1992)
38 T.R. Ohno, Y. Chen, S.E. Harvey, G.H. Kroll, J.H. Weaver, R.E. Haufler, R.E. Smalley: Phys. Rev. B **44**, 13 747 (1991)
39 E. Rotenberg, C. Enkvist, P.A. Brühwiler, A.J. Maxwell, N. Mårtensson: Phys. Rev. B **54**, R 5279 (1996)